Proc. of the Intl. MEDCOAST Conference on Wind and Wave Climate of Mediterranean and Black Sea,
***WIND & WAVE CLIMATE '99**, March 30 - April 2, 1999; Antalya, Turkey. Abdalla, Özhan (Editors)*

Sea-21 Forecasting Operability of Marine Installations

Michael Stiassnie and Michael Glozman

Coastal and Marine Engineering Research Institute
Technion City Haifa 32000, Israel
Tel: 972-4-8220642, Fax: 972-4-8227661,
E-mail: michael@cameri2.technion.ac.il

Abstract

Forecasting operability conditions of marine installations requires sophisticated software packages, based on up-to-date knowledge of nonlinear water-wave theories. *Sea-21* is CAMERI's most recent answer to this engineering challenge. The present note contains simplified explanations of the most relevant physical processes that affect the quality of loading/unloading conditions of ships in harbors. Simple calculations provide approximate results, which indicate the importance of appropriate handling of near-resonant conditions.

Introduction

Harbors are built to provide shelter for ships, and to enable undisturbed cargo handling almost constantly. However, many harbors are connected by their entrance to the open sea, and parts of their interior waters undergo significant motions in stormy weather conditions. The motion of the water affects the berthed ships, which quite often have eigen-frequencies similar to those of the harbor and to the frequencies of the forcing long-waves.

The occasional fierce motion of the moored ships (depending on its severity) may interrupt, or stop, the cargo handling, may force the ship to leave the berth, or even result in damage to the ship and quay. It is clear that advanced knowledge regarding the quality of cargo handling conditions (good, bad, or dangerous) will significantly improve the decision making process of harbor masters. CAMERI, the Israeli Coastal and Marine

Engineering Research Institute has developed a software package called ***Sea-21***, with the aim to provide such information for up to 48 hours in advance.

The pilot version of ***Sea-21*** is installed at the Haifa harbor. A detailed demonstration of a working system, identical to the one installed in Haifa, is an integral part of the oral presentation. The details of the mathematical formulation and of the technical aspects of ***Sea-21*** were summarized in a paper which is included in the Proceedings of the 5th International Workshop on Wave Hindcasting and Forecasting, Melbourne, Florida, January 1998; copies of this paper are available upon request. The aim of this note is to demonstrate, by means of a rather simplified example, some of the main physical processes, which determine the quality of operability conditions.

General Layout

Fig. 1 shows a ship moored in an inner basin, which is protected by a breakwater. The depth of the harbor (and its close vicinity) h is constant. The outer depth contours are parallel to the breakwater. The main geometrical parameters of the harbor are:

l_{12} – the distance between head of breakwater and the basin-entrance
l_{23} – the distance between the basin-entrance and the ship
l_{24} – the length of the inner basin
θ_{12} – angle between the l_{12} line and the breakwater

Wind waves with frequency ω, period $T_S = 2\pi/\omega$ and deep-water amplitude a_0 attack the system perpendicular to the depth contours ($\theta_0 = \pi/2$). To follow the physical processes from the waves in deep water up to the surge motion of the ship, we adopt the following notation:

- The area near the breakwater head is denoted by subscript 1
- The area near the entrance of the inner-basin is denoted by subscript 2
- The vicinity of the ship is denoted by subscript 3
- The far end of the inner basin is denoted by subscript 4

The main physical processes are: shoaling and generation of ***long-waves***, diffraction around the breakwater head, agitation of the inner-basins, and surge motion of the ship.

Shoaling and Generation of Long-Waves

Linear shoaling theory gives the wave amplitude near the harbor entrance by

$$a_1 = \left(\frac{g}{2\omega c_{g1}}\right) a_0 \qquad (1)$$

where g is the acceleration of gravity and c_{g1} is the group velocity

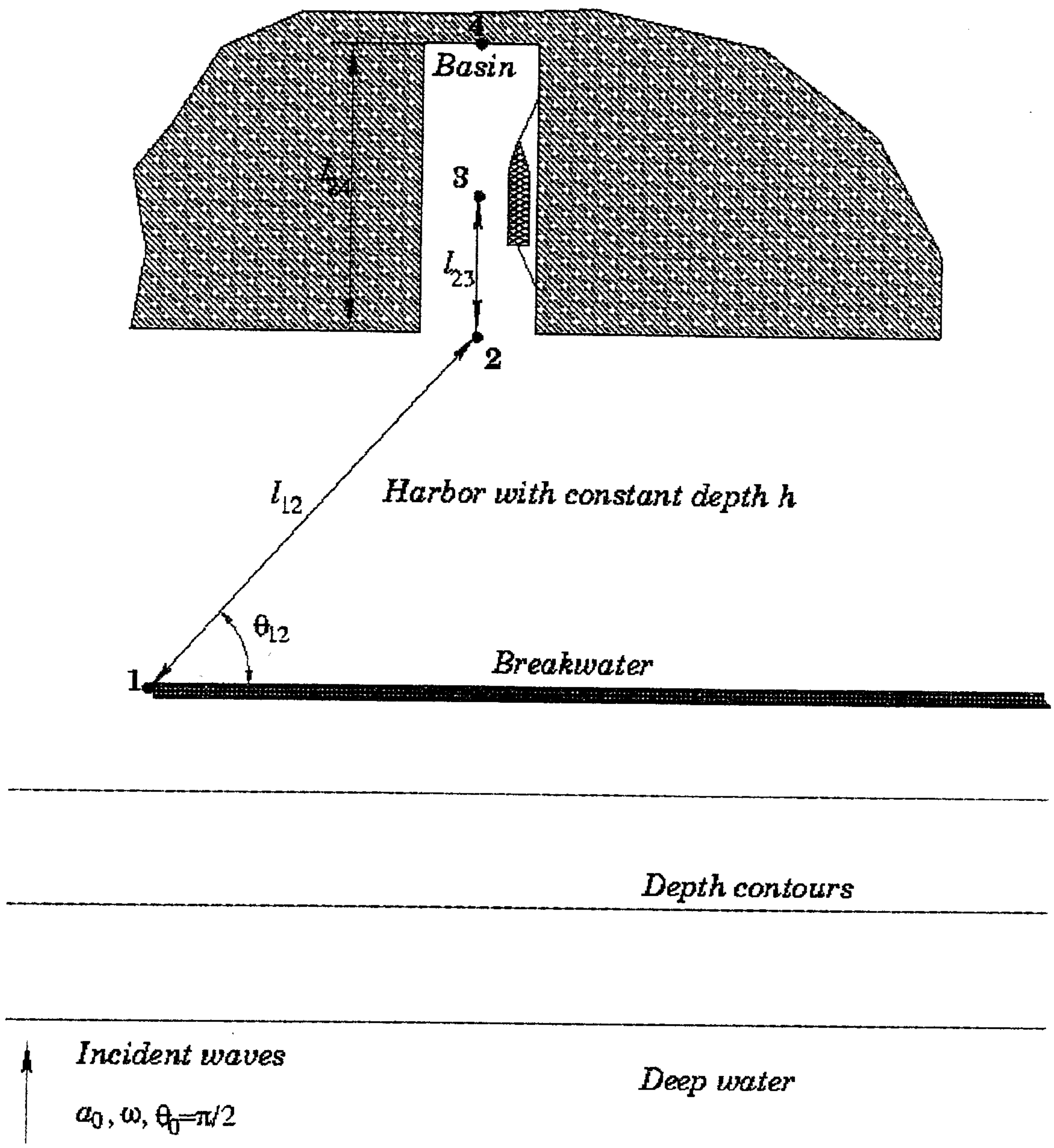

Fig. 1: Layout of the simplified example.

$$c_{g1} = \frac{\omega}{2k_1}\left(1 + \frac{2k_1 h}{\sinh(2k_1 h)}\right) \tag{2}$$

The wave-number k_1 is related to the frequency ω and depth h through the dispersion relation

$$\omega^2 = gk_1 \tanh(k_1 h) \tag{3}$$

It is well known that water-waves are affected by side-band instability, which introduces an additional wavelength into the system. These waves are much longer than the wind-waves, and are referred to as 'long-waves'. The most unstable side-band mode produces a long-wave with frequency Ω given by:

$$\frac{\Omega}{\omega} = \frac{a_0 \omega^2}{g} \tag{4}$$

Note that both frequencies, ω – for the wind-waves, and Ω – for the long-waves, remain unchanged through all subsequent physical processes. In Eq. (4) and in the sequel, quantities related to the wind/long waves are denoted by ordinary/capital letters, respectively.

The amplitude of the long-waves at the harbor entrance is (See Stiassnie (1983)).

$$A_1 = \frac{g}{8}\left(\frac{4k_1 c_{g1}}{\omega} - 1\right)\frac{a_1^2}{gh - c_{g1}^2} \tag{5}$$

Diffraction by Breakwater

The waves at the entrance to the inner-basin are calculated by the theory of linear diffraction by a semi-infinite breakwater, see Wiegel (1964).

$$a_2 = |\psi|\, a_1 \;,\; A_2 = |\Psi|\, A_1 \tag{6a,b}$$

where

$$\psi = 0.5\{1 + C(\zeta) + S(\zeta) + i[C(\zeta) - S(\zeta)]\}e^{-ik_1\ell_{12}\cos(\theta_{12}-\theta_0)} + \\ + 0.5\{1 + C(\zeta') + S(\zeta') + i[C(\zeta') - S(\zeta')]\}e^{-ik_1\ell_{12}\cos(\theta_{12}+\theta_0)} \tag{7}$$

Here, C, S are the Fresnel integrals and

$$\zeta = 2\sqrt{\frac{k_1\ell_{12}}{\pi}}\sin\left[\frac{1}{2}(\theta_{12} - \theta_0)\right]; \quad \zeta' = -2\sqrt{\frac{k_1\ell_{12}}{\pi}}\sin\left[\frac{1}{2}(\theta_{12} + \theta_0)\right] \tag{8a,b}$$

To obtain Ψ, one has to replace k_1 in the above equations by $K_1 = \Omega/\sqrt{gh}$.

Agitation in the Inner-Basin

To find the waves, which attack the ship, we assume perfect reflection from the end of the basin, which yields

$$\frac{a_3}{a_2} = \frac{\cos[k_1(\ell_{24} - \ell_{23})]}{\cos k_1 \ell_{24}}, \quad \frac{A_3}{A_2} = \frac{\cos[K_1(\ell_{24} - \ell_{23})]}{\cos K_1 \ell_{24}} \tag{9a,b}$$

Note that when the argument of the cosine function in the denominator equals $(2n - 1)\pi/2$, $n = 1,2,...$ (i.e., Ω is equal to an eigen-frequency of the basin), the basin resonates and a more accurate theory is needed (see Appendix A). The amplitudes at the far end of the basin (point 4), are obtained from (9a,b), when the cosines in the numerators are replaced by one.

Motion of Ship

We concentrate on the motion of the ship along the quay, called surge. The width of the ship is B and its draft - D. The mass of the ship is m, and the along-the-quay linear spring-constant of the mooring lines is s. The surge amplitudes of the ship are found by solving its equation of motion and are given by:

$$x = F_s / |m\omega^2 - s|; \quad X = F_l / |m\Omega^2 - s| \tag{10a,b}$$

where the order of magnitude of the force that the wind waves exert on the ship is estimated through the integration of pressure on the rectangular B (the ships' width) times D (its draft):

$$F_s = \frac{\rho\omega^2 |a_3| B}{k_1^2} \left\{ 1 - \frac{\sinh[k_1(h - D)]}{\sinh[k_1 h]} \right\} \tag{11}$$

where ρ is the density of the water.

The force of the long-waves is obtained from the so-called Froude-Krylov hypothesis

$$F_l = mgK_1 \left| \frac{\sin[K_1(\ell_{24} - \ell_{23})]}{\cos(K_1 \ell_{24})} \right| \tag{12}$$

When the denominators in Eq. (10a,b) tend to zero, i.e., when Ω tends to the eigen-frequency of the ship and its mooring system, and resonance conditions are approached, more accurate approximations are required (see Appendix B).

Operability Condition

When the surge amplitude X (which is usually much larger than x) exceeds certain thresholds the operability condition deteriorate. One can regard the following values as a rough guideline.

- $X < 0.5$ m - good conditions
- 0.5 m $< X < 1$ m - difficult conditions
- 1 m $< X < 2$ m - bad to extremely bad conditions
- 2 m $< X$ - dangerous conditions

As a numerical example, we choose the case given in Table 1, where $T_l = 2\pi / \Omega$ is the period of the long-waves.

Table 1: Parameters for the numerical example

Parameter	h, m	T_s, sec	T_l, sec	a_0, m	θ_{12}, deg	l_{12}, m	l_{23}, m	l_{24}, m
Value	12	8	63.6	2	45	1000	800	400
Parameter	m, kg	B, m	D, m	s, N/m	a_1, m	a_2, m	a_3, m	a_4, m
Value	$4 \cdot 10^7$	30	10	$5 \cdot 10^5$	1.69	0.14	0.02	0.14
Parameter	A_1, m	A_2, m	A_3, m	A_4, m	F_s, N	x, m	F_l, N	X, m
Value	0.12	0.03	0.04	0.05	$4.9 \cdot 10^4$	0.002	$8.7 \cdot 10^4$	0.79

Note that the breakwater provides a much better shelter against the short wind waves than against the long waves ($a_2 / a_1 < A_2 / A_1$).

For this case the forces acting on the ship by short and long waves, are of comparable order of magnitude, but yield very different surge amplitudes. The fact that similar forces lead to so significantly different surge amplitudes is related to the ratio Ω / ω. For the case at hand, the operability conditions are in the difficult range.

Two Avenues to Resonance

- When the length of the inner-basin in the former example is increased to l_{24} = 1200 m without changing any of the other parameters, Ω approaches one of the eigen-frequencies of the basin ($2K_1 l_{24} / \pi = 6.96$ for l_{24} = 1200 m, compared to 4.64 for l_{24} = 800 m). This causes currents about 6 times stronger than before and yields $X = 10.6$ m (x = 0.03 m). As a result, frictional effects in the basin become significant (see Appendix A) and, when taken into account, reduce the amplitude to less than half of the above value.

- The stiffness of the mooring system has also a profound influence of the motion. Table 2 gives the values of X for different s, without any other change of the original case (l_{24} = 800 m). The dimensionless parameter $m\Omega^2/s$ is also shown, since its proximity to one indicates resonant conditions of the ship-mooring configuration.

For $s = 3.8 \cdot 10^5$ N/m, the rather large linear results for the motions indicate that the non-linear properties of the mooring system have to be taken into account (see Appendix B). When $\tilde{s} = 3 \cdot 10^4$ N/m, which is a plausible value, is substituted into (17) one gets $X = 1.57$ m, which is significantly smaller than the above 8.52 m.

Table 2: Influence of mooring stiffness on motion of a moored ship.

s, N / m	$m\Omega^2 / s$	X, m	Comments
0	∞	0.22	free motion
$1 \cdot 10^5$	3.9	0.30	weak mooring
$3.8 \cdot 10^5$	1.02	8.52	close to resonance
$5 \cdot 10^5$	0.78	0.79	original example
$1 \cdot 10^6$	0.39	0.14	stiff mooring

Conclusion

In reality the bathymetry contours are not parallel, the breakwaters are not straight, the harbor layout can be complex, and its depth is not necessarily constant. The attacking storms depend on local and distant weather conditions and have usually broad spectra. The motion of a moored ship in six degrees of freedom is affected by its own geometry, as well as by proximity of the quay. All of the above parameters are incorporated into the different mathematical modules of ***Sea-21*** system and controlled by its user-friendly interface to provide an accurate operability forecast for up to 48 hours in advance.

References

Dean, R.G. and Dalrymple, R.A. (1984). "Water Wave Mechanics for Engineers and Scientists", World Scientific, 353 p.

Nayfeh, A.H. (1981). "Introduction to Perturbation Techniques", John Wiley & Sons, 513 p.

Stiassnie, M. (1983). "Derivation of the Nonlinear Schrodinger Equation for Shoaling Wave Group", J. of Applied Mathematics and Physics (ZAMP), 34, 534-544.

Wiege, R.L. (1964). "Oceanographical Engineering", Prentice-Hall, 532 p.

Appendix A. Resonance of Inner-basin

When $2K_1l_{24} / \pi$ is close to an integer, A_3 in (9b) becomes very large and bottom friction starts to play an important role. Following Dean and Dalrymple (1994) equation (9b) is replaced by

$$\frac{A_3}{A_2} = \left\{ \frac{\cosh^2 K_i\ell_{34} \cos^2 K_r\ell_{34} + \sinh^2 K_i\ell_{34} \sin^2 K_r\ell_{34}}{\cosh^2 K_i\ell_{24} - \sin^2 K_r\ell_{24}} \right\}^{1/2} \tag{13}$$

where $l_{34} = l_{24} - l_{23}$,

$$K_r = \frac{\Omega}{\sqrt{2gh}} \left[\sqrt{1 + \left(\frac{\alpha}{\Omega}\right)^2} + 1 \right]^{1/2} \; ; \; K_i = \frac{\Omega}{\sqrt{2gh}} \left[\sqrt{1 + \left(\frac{\alpha}{\Omega}\right)^2} - 1 \right]^{1/2} \tag{14a,b}$$

and α, typically a small number, is given by

$$\alpha = \frac{fg^{1/2} A_3}{3\pi h^{3/2}} \tag{15}$$

where f is the Darcy-Weisbach friction factor. For $\alpha = 0$, also $K_i = 0$ and (13) reduces to (9b). Note that for $\alpha > 0$ the denominator of (13) is always positive.

Appendix B. Resonance of Moored Ship

When Ω approaches $\sqrt{s/m}$, one can see from (10b) that X diverges. When X gets large enough the nonlinear property of the mooring system becomes important, and the dynamics of the ship can be then studied as forced oscillations of the Duffing equation. From Nayfeh (1981), for weak nonlinearity, (10b) is replaced by the solution of the cubic equation

$$\frac{3}{8} X^3 - \left(\Omega \sqrt{\frac{m}{s}} - 1 \right) \frac{s}{\tilde{s}} X = \frac{F_l}{2\tilde{s}} \tag{16}$$

where the force in the mooring system is given by the cubic polynomial $sX + \tilde{s}X^3$.

When $\tilde{s}X^3 << sX$, (16) yields (10b). However, at 'resonance', X is finite and given by

$$X \approx \left(\frac{4F_l}{3\tilde{s}} \right)^{1/3} \tag{17}$$

For finite (not weak) nonlinearity, the Duffing equation produces a wealth of solutions, including chaotic ones.